High resolution transmission electron microscopic in-situ observations of plastic deformation of compressed nanocrystalline gold

Guoyong Wang, Jianshe Lian, Qing Jiang, Sheng Sun, and Tong-Yi Zhang

Citation: Journal of Applied Physics **116**, 103518 (2014); doi: 10.1063/1.4895550
View online: http://dx.doi.org/10.1063/1.4895550
View Table of Contents: http://scitation.aip.org/content/aip/journal/jap/116/10?ver=pdfcov
Published by the AIP Publishing

High resolution transmission electron microscopic *in-situ* observations of plastic deformation of compressed nanocrystalline gold

Guoyong Wang,[1] Jianshe Lian,[1] Qing Jiang,[1] Sheng Sun,[2] and Tong-Yi Zhang[2,a)]
[1]*Key Laboratory of Automobile Materials, Department of Materials Science and Engineering, Jilin University, No. 5988 Renmin Street, Changchun 130025, People's Republic of China*
[2]*Department of Mechanical Engineering, Hong Kong University of Science and Technology, Clear Water Bay, Kowloon, Hong Kong Special Administrative Region*

(Received 22 June 2014; accepted 1 September 2014; published online 12 September 2014)

Nanocrystalline (nc) metals possess extremely high strength, while their capability to deform plastically has been debated for decades. Low ductility has hitherto been considered an intrinsic behavior for most nc metals, due to the lack of five independent slip systems actively operating during deformation in each nanograin. Here we report *in situ* high resolution transmission electron microscopic (HRTEM) observations of deformation process of nc gold under compression, showing the excellent ductility of individual and aggregate nanograins. Compression causes permanent change in the profile of individual nanograins, which is mediated by dislocation slip and grain rotation. The high rate of grain boundary sliding and large extent of widely exited grain rotation may meet the boundary compatibility requirements during plastic deformation. The *in situ* HRTEM observations suggest that nc gold is not intrinsically brittle under compressive loading. [http://dx.doi.org/10.1063/1.4895550]

INTRODUCTION

Nanocrystalline (nc) metallic materials have been expected as next generation of advanced structure materials for decades.[1] Ideally, nc metals should possess ultra-high strength, as indicated by the Hall-Petch relationship that the strength is inversely proportional to the square root of grain size, and ultra-high ductility according to Gleiter and co-worker's prediction.[2,3] Although the inverse Hall-Petch relationship has been found in many nc metals when grain size decreases below 10 nm, these nc metals have already reached extremely high strengths compared to their coarse-grained counterparts.[4,5] This means the strength of nc metals has already met the requirement of advanced structure materials. In contrast, the ductility of nc metals during tensile tests is generally lower than their coarse-grained counterparts.[5] On the other hand, the superplastic behavior has been observed in nc nickel and metal alloys at room temperature,[6] which brings a bright prospect of nc metals as potential advanced structure materials. More and more intensive research on mechanisms of plastic deformation of nc metals has been carried out with various theoretical, numerical, and experimental approaches, such as Molecular dynamics (MD) simulations,[7,8] theoretical modeling and calculations,[9–11] postmortem and *in-situ* transmission electron microscopic (TEM) observations,[12–14] and compression and tension tests at different strain rate.[15,16] The discovered and/or suggested deformation mechanisms in nc metals include grain boundary (GB) sliding/migration,[16,17] grain rotation,[9–11,14] GB diffusion,[15,18] dislocation source vanishing inside nanograins and extended dislocation nucleation from GBs,[12,13,19,20] which clarify, to a large extent, the origination and physical pictures of plastic deformation in nc metals. In spite of the great progress, it is still unclear whether nc metals are intrinsically brittle or ductile. Are these discovered and/or suggested deformation mechanisms really unable to accomplish large plastic deformation in nc metals?

A bulk nc metal sample generally consist of millions of nanograins and plenty of GBs between them. Its ductility is heavily determined by the capability of each nanograin to deform plastically and the deformation compatibility in all involved nanograins and GBs. Recently, a lot of *in-situ* TEM experiments have been carried out on individual metallic nanopillars and nanowires.[21,22] These samples, nanopillars and nanowires, are totally made of single crystal or bicrystal and the size of the sample is close to the nc grain. Thus, the results of these experiments inspire the understanding of the plastic deformation behavior of the nc grain in bulk nc metals. Interestingly, the plastic deformation behavior of nanopillar and nanowires show considerable difference to their bulk counterparts. As the diameter of the nanopillar and nanowires decreases, the yield strength increases following the normal Hall-Petch relationship[23,24] and especially, the strength raise much sharply to near the theoretical strength when the diameter falls below a critical size. The inverse Hall-Petch relationship has not been observed in the mechanical testing of nanopillars/nanowires. Furthermore, the small volume single crystals during tensile tests exhibit fantastic ductility, large plasticity or super-plasticity, while their bulk counterparts are brittle.[25–27] These experiments illumine our limitless hope to pursuit for high ductile nc materials, because a metallic nanograin might be deformed as plastically as the nanopillar/nanowire. If plastic deformations in all nanograins of a bulk nc metal is compatible with GB deformation, crack nucleation from GBs will be suppressed and nc metal will have a good ductility. The goal of the present work is to investigate the capability of plastic

a)Author to whom correspondence should be addressed. Electronic mail: mezhangt@ust.hk. Tel.: (852) 2358-7192. Fax: (852) 2358-1543.

deformation of individual nanograin and the compatibility of the intragranular and intergranular deformation in bulk nc metal. For this purpose, we design and conduct an experiment to *in situ* observe the deformation process of the nanograins and GBs in a nc gold under compression.

EXPERIMENTAL DETAILS

A dozen of copper wires with a diameter of 0.8 mm and 10 mm length and a silicon sheet were firstly rinsed with ethanol in ultrosonator for 5 min. The clean wires were placed on the sheet, and then both of them were put into a Gold Coater (Scancoat Six, Edwards) to sputter gold for 15 s. After that, one Au-coated wire was selected and loaded on a TEM-AFM holder (Nanofactory) and the holder was installed inside a JEM 2010 HRTEM (JEOL) chamber. The TEM was operated at 200 kV working voltage. The margin of the gold film is thin enough for TEM observation. Fig. 1 shows that the gold film consists of millions of nanograins with diameter ranging from 3 to 5 nm. Thus, when the AFM Tip with a diameter around 100 nm was pushed to compress the Au film, the deformation process of some grains was observed and recorded *in situ* by HRTEM.

RESULTS

Deformation of nanograins

The white arrow in Fig. 2(a) indicates a nanograin with interference fringes, while the black arrow there shows the loading direction. The fringe spacing is 0.235 nm, corresponding to the (111) planar spacing of face-centered cubic (fcc) Au crystal based on the XRD PDF card of PDF-#:65-2870. The crystal structure evolution of the nanograin during the compressive test was record by CCD camera. Fig. 2(b) is a HRTEM image after the compression, illustrating that the left up half edge of the nanograin was declined towards the right side and the atomic layers there were homogeneously sheared layer by layer towards the right side. The topmost atom layer was moved about 2.2 nm away to the right side, corresponding to a shear strain 0.6 as the compressed crystal is only 3.7 nm

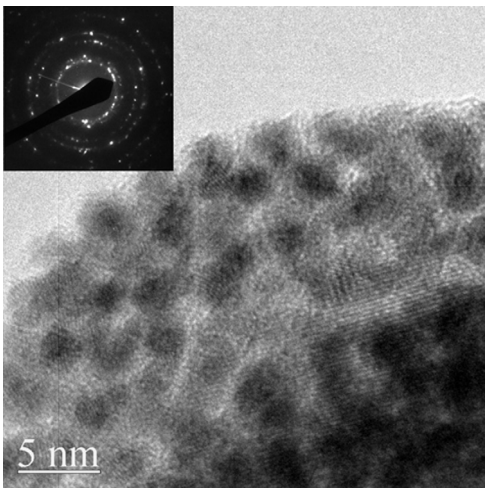

FIG. 1. A TEM image showing the microstructure of the nc gold coated a copper wire. It is composed of many nanograins with a diameter ranging 3–5 nm. The inset is the corresponding SAD pattern.

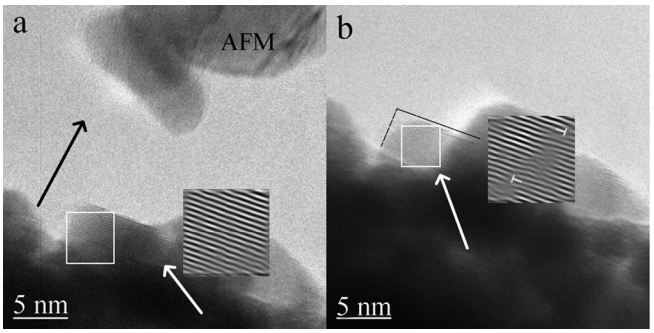

FIG. 2. A HRTEM images of a grain protruded from the surface (a). The inset is the Fast Fourier Transform image of the grain, showing no dislocation there. The black arrow indicates the compression direction. After compression, the deformed grain was characterized by the HRTEM image of (b). The inset is the corresponding Fast Fourier Transform image, showing two residual dislocations inside the grain after compression. The white square boxes in Figs. 2(a) and 2(b) indicate the regions of the Fast Fourier Transform images. The contour line of the grain before compression is added in (b) to make the deformation clear. (Multimedia view) [URL: http://dx.doi.org/10.1063/1.4895550.1]

in high. The insets in Figs. 2(a) and 2(b) are, respectively, the Fast Fourier Transform (FFT) images of the grain before and after compression. None dislocation is found in the inset of Fig. 2(a) and two dislocations appear in the inset of Fig. 2(b). Obviously, dislocation sliding was involved in the plastic deformation and the dislocations denoted in the inset of Fig. 2(b) belonged to a same slip system. It is well-known that single slip in single crystal always leads to an inerratic contour, while multiple slip always leads to a smooth and erratic contour. Based on the contour and the FFT inset analysis, it suggested that only single slip was activated in the compressed grain. Figs. 3(a) and 3(b) are HRTEM images before and after the compressive test on another nanograin, where the insets are the corresponding FFT images. The interference fringe pattern of Au (111) planes with plane spacing of 0.235 nm was clearly observed by HRTEM during compression. After the compression, the grain was plastically deformed about 0.5 in shear strain. It is clearly shown in the inset of Fig. 3(a) that there is no dislocation inside the grain before compression. But, three dislocations, one individual dislocation and a dislocation dipole, are found inside the deformed grain after compression, as shown by the inset of Fig. 3(b). The individual dislocation is near the surface and the dipole is at the bottom of the grain. Obviously, the three dislocations were located on two different atomic planes. Multiple slip may be activated in this grain. But, according to the contour changing and the FFT inset analysis, the number of independent slip systems simultaneously activated in the grain was still very less, far from five. It is noticeable that the dipole located region shows high diffraction contrast, which could be induced by strain field of dislocations. Such high diffraction contrast shows up frequently in the course of the compression test, as evidenced in the video. In addition to the dislocation strain field, bending contour and crystal rotation can also cause changes in diffraction contrast. The bending contours often come with pairs and move like water-wave in a diffused and curved manner, as shown in the picture at 10 s of the video. The bending contour may be caused by the compression which results in the distorting or bending of the grain. Crystal rotation changes the

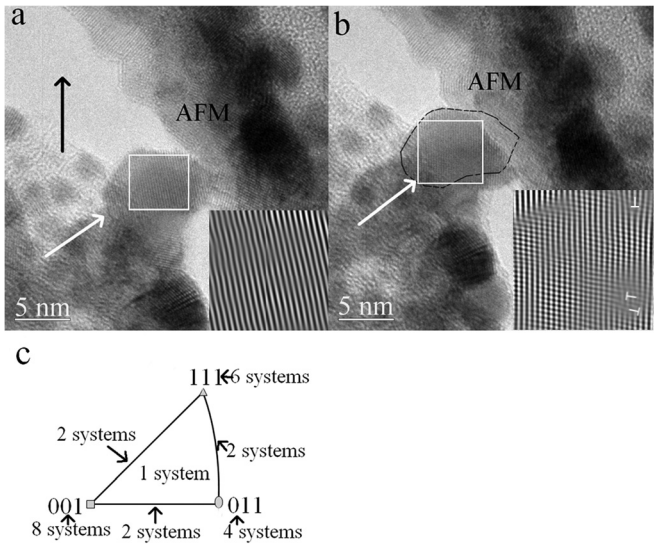

FIG. 3. HRTEM images of another grain before (a) and after compression (b). The black arrow denotes the moving direction of the sample. The contour line of the grain before compression is also added in (b). The insets in (a) and (b) are the FFT images of the grain before and after compression from the white square boxes, showing that a residual single dislocation and a residual dislocation dipole were in the deformed grain after the compression. (c) The standard triangle of the [001] stereographic projection of a cubic crystal. For an fcc metal, single slip is obtained for crystals whose orientations are located within the standard triangle. Duplex slip occurs for crystals with orientations lying along the triangle perimeter, and even more slip systems operate when [001], [011], [$\bar{1}$11] directions are parallel to the stress axis. (Multimedia view) [URL: http://dx.doi.org/10.1063/1.4895550.2]

orientation of the grain and the diffraction contrast pattern entirely, as shown in the picture at 24 s of the video. The most observed change in diffraction contrast occurs firstly in part of the grain and then slowly penetrates through the grain. This kind of change in diffraction contrast might be attributed to dislocation sliding. The grain rotation here might be related to GB sliding between the grain and the substrate. Of course, the orientation of a crystal can also be changed by intragranular plasticity, such as successive dislocation sliding on neighbor parallel slip planes. If it happened, the grain's diffraction contrast would be changed step by step, differing from the view at 24 s of the video. In general, surface nanograins must behave different from bulk nanograins located at the interior of a bulk sample. This is because surface nanograins have much less mechanical constraints. The capability of emitting dislocations from a surface or GB highly depends on the atomic structure of the surface, such as steps and roughness, where stress concentration occurs, and the GB structure, where GB dislocations may exist. Surfaces have a stronger ability than GBs to attract and absorb dislocations due the larger elastic mismatch of solid/vacuum than that of solid/solid. Comparing the images before and after compression in Figs. 2 and 3, it is clear that the lengths of the slipped (111) planes remain unchanged. Especially, the ratio of the plane length to the crystal height remains unchanged. The experimental observations might exclude the possibility of diffusion-mediated reshaping which should greatly change the length of atom plane and the ratio by mass transfer between different atom planes and locations. The outmost (111) plane of the crystal shown in Fig. 2(a) is very short in comparison with the interior (111) planes. If diffusion were predominant during the deformation, this outmost (111) plane would become even shorter until disappearing due to the applied stress field. However, this (111) plane is still there after the test and maintains the same length, as shown in Fig. 2(b). Although the low spatial resolution in the videos hardly provide the synchronous details of dislocation configuration, the residual dislocations in the deformed grains of Figs. 2(b) and 3(b) might prove that dislocation sliding dominates the plastic deformation. Fig. 3(c) indicates that how many slip systems will be operated in a fcc crystal under an uniaxial compressive stress, where the stress is applied along different crystal orientation. The six and eight slip systems will be actively operated when the stress is applied along the ⟨111⟩ and ⟨100⟩ directions, respectively. For single nanocrystals, the possibility to act single slip system is much larger than to act multiple slip systems. The three residual dislocations in Fig. 3(b) are obviously on different slip planes. Although we did not analyze the stress field in the two surface nanograins, which must differ from that in a bulk single crystal under uniaxial compression, the HRTEM observations might indicate that less than five independent slip systems were activated simultaneously during the plastic deformation in these surface nanograins, which has to lead to relative displacements across GB. This might be reasonable because the grain size is so small at the nanometer scale. The likelihood for dislocation pile-up and intersection becomes smaller in nanograins. As indicated in the MD simulations,[7] dislocations tend to be emitted from GBs, travel trough the tiny grains quickly and then be absorbed by the opposite GBs in such small nanograins. Recently, *in-situ* TEM observations on Pt ultrathin film with nanometer grains show that for the larger grains ($d \sim 10$ nm), full dislocations dominate the plastic deformation behavior and their evolution sometimes leads to the formation, destruction, and reformation of Lomer locks. In smaller grains ($d < 10$ nm), partial dislocations generating stacking faults are prevalent.[28] Therefore, the dislocation activity is still an essential mechanism in plastic deformation of nanograins, although the active slip systems might be less than five in each nanograin, which does not meet the compatibility requirement across GBs. Thus relative displacements should happen across GB. If the relative displacements can be completed by GB sliding rather than void or overlap, the plastic deformation still can continue. Or, fracture will terminate the deformation.

The GB sliding

The HRTEM image in Fig. 4(a) shows a crystal with a diameter of about 20 nm on the substrate, where the interference fringe patterns of the crystal (200) and the substrate (111) are both clearly observed. During compression, the relative slip occurred between the crystal and the substrate and the process was recorded. The crystal was pushed downwards and hidden behind the substrate during compression. Then we stopped compressing and withdrew the tip back. The crystal was also pulled out because of the attractive force between it and the AFM tip. When the crystal was separated from the AFM tip, it almost returned to the original place, as shown in Fig. 4(b), but its orientation has changed,

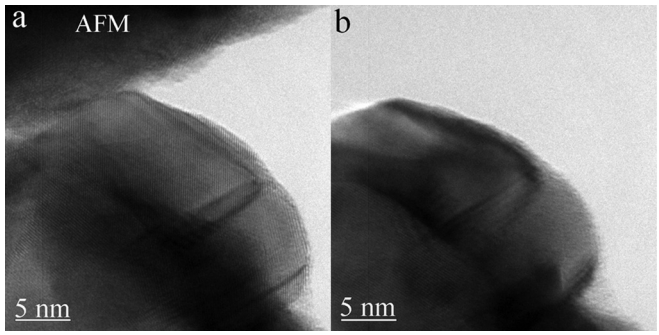

FIG. 4. (a) A HRTEM image of a big gold grain deposited on a grain of the Cu substrate. Both interference fringes of the grain and the substrate were clearly shown in the image, which can indirectly ascertain the relative orientation of them. (a) A HRTEM image of the grain after compression. The fringe of the substrate indicates the compression had little effect on the substrate orientation, while the grain orientation changed and its original fringe was lost. (Multimedia view) [URL: http://dx.doi.org/10.1063/1.4895550.3]

as proved by the disappearance of its fringe, while the fringe of the substrate remained unchanged. The restoration process confirms that it is GB sliding that completes the displacement. The grain did not break off from the substrate and it was still linked by GB. Or it should be attached on the AFM tip rather than restoration as the tip departed from the nc gold. The pushing-in and pulling-out process took nearly 3 min. Thus, the average sliding velocity of the grain relative to the substrate (GB sliding velocity) can be estimated as about 2×10^{-10} m/s, which is lower than but close to the dislocation velocity at yielding.[29] In fact, this velocity is high enough to mediate the GB mismatch induced by dislocations. Only a step of one Burgers vector can be generated as a dislocation is absorbed by GB after it slides through the whole grain. During the pushing and pulling process, the variation of diffraction contrast always starts from one end and moves to the other, which might be an indicator of dislocation sliding. Carefully comparing the images of Figs. 4(a) and 4(b) shows almost the same shape of the bulk nanograin before and after the compression, which is completely different from the deformation behavior of surface nanograins. This result implies that GB can slide at an appropriate velocity, which is expected to match the relative displacement across GB.

HRTEM is very sensitive to the orientation of lattice relative to electron beam. A clear interference fringe is formed only when the electron beam parallels with a zone axis of crystallographic lattice. This character of HRTEM is used here to detect grain rotation during compression. A region of several nanograins was selected during the compressive test and the movement of each grain in this region was in situ recorded by HRTEM. Fig. 5 shows a series of representative images. Very luckily, we found a grain, named as grain A, shown in the center of Fig. 5(a). The interference fringe of grain A appeared all time during the deformation process. Thus, grain A was taken as reference to study the rotation of other grains. Fig. 5(a) also shows HRTEM interference fringe of another grain, called grain B, on the lower left side of grain A. As the compression went on, grain B's fringe disappeared, as shown in Fig. 5(b), while grain A's fringe

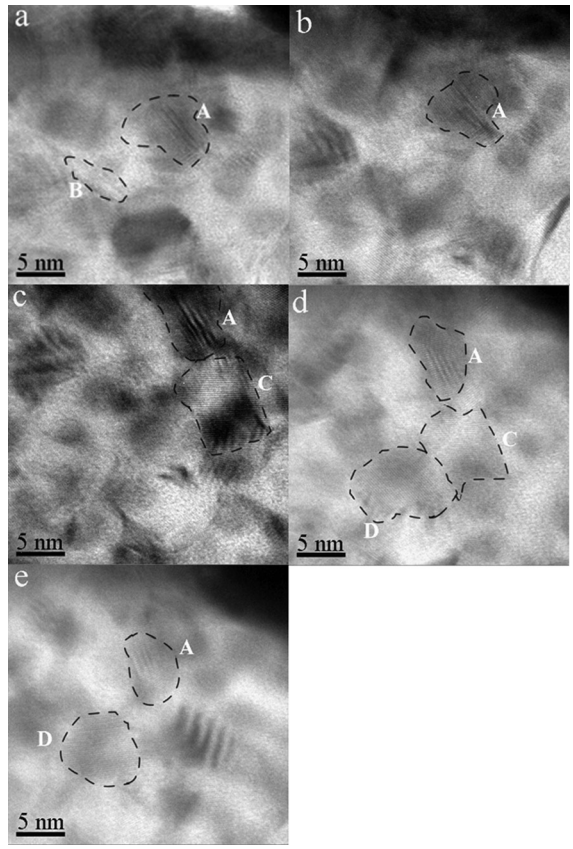

FIG. 5. HRTEM images of an nc gold protrusion under mimic compressive test by a AFM tip (a)–(e). A interference fringe of a grain, called grain A, was clearly shown in (a), and this fringe was always shown there during the compression, which makes sure that the protrusion did not rotate or tilt during compression. The following observed moved of the grains should originate from deformation. Many other grain's interference fringes appeared and then disappeared during compression (a)–(e), which proves the grain rotation widely exists in nc gold during deformation. (Multimedia view) [URL: http://dx.doi.org/10.1063/1.4895550.4]

remained unchanged. This is a direct evidence of the rotation of grain B relative to grain A. Similar phenomena were also observed on other grains, grain C just beneath grain A, and grain D on the left side of grain C. Grains C and D did not show any interference fringes in Fig. 5(a), whereas grain C showed its interference fringe in Fig. 5(c) and grain D showed its interference fringe in Fig. 5(d). As deformation going on, the fringe of grain C disappeared and the interference plane was transformed in grain D, as shown in Fig. 5(e). Grain D shows clearly the (111) plane interference fringe at the moment of Fig. 5(d) and the (200) plane fringe at the moment of Fig. 5(e). The rotation angle of grain D is about 55°, which occurred in about 12 s. The *in situ* observations lead to the conclusion that grain rotation is a very common deformation mechanism in the nc gold during compressive deformation. The experiment results are consistent with MD simulations.[30] Texturing of ductile coarse-grained metals after cold working indicate that coarse grains can rotate their orientations with the help of dislocation activity, where more than five slip systems are operated in each coarse grain due to the large grain size. However, the active slip systems might be less than five in each nanograin due to the small grain size, as proved by aforementioned

experiment. No voids or cracks appeared around the rotated grain, as shown in Fig. 5. The deformation compatibility must be satisfied by the GB sliding. As observed in this experiment, grain rotation wildly exists in the region suffering compressive deformation. That strongly suggests GB sliding can happen between any deformed adjoining nanograins where the mismatching displacement was induced by dislocation slips in each grain. While GB sliding is able to mediate the mismatching across GB, it is also very effective to suppress the formation of voids and cracks which always lead to the end of plastic deformation.

CONCLUSION

In summary, the nc gold grains have been testified by the HRTEM *in situ* observations in our experiment that they still have the ability to suffer large plastic deformation under compression. But the deformation is completed by very less slip systems, which obviously indicates that it is hard for nc metals to simultaneously have the operation of five independent slip systems to match the displacement across GB between adjoining deformed grains. The present HRTEM observations indicate that GBs can slide at an appropriate rate comparable to dislocation slip. Thus, GBs in nanograined metals have the ability to mediate the mismatching between nanograins induced by dislocation slip, which avoids cracking. Meanwhile GB sliding was testified in this experiment to wildly exist between any deformed adjoining nanograins, for nanograin rotation motivated by GB sliding was observed to act in a compressive grain aggregate. Therefore, nc metals are not intrinsically brittle. The disappointingly low tensile strain should relate to the disappearance of the macroscopic work-hardening capacity of nc metals. Large plastic strain is still expected in nc metal under other deformation method, such as compression, high pressure torsion, and even rolling, at an appropriate strain rate.

ACKNOWLEDGMENTS

The project was supported by a general research grant (#622911) from the Hong Kong Research Grants Council, Hong Kong, China and the Foundation of National Key Basic Research and Development Program (No. 2010CB631001), National Nature Science Foundations (Grant No. 51401083 and No. 51371089), the Program for Changjiang Scholars and Innovative Research Team in University.

[1]K. Lu, Science **328**, 319–320 (2010).
[2]J. Karch, R. Birringer, and H. Gleiter, Nature **330**, 556–558 (1987).
[3]A. H. Chokshi, A. Rosen, J. Karch, and H. Gleiter, Scr. Metall. **23**, 1679–1683 (1989).
[4]C. E. Carlton and P. J. Ferreira, Acta Mater. **55**, 3749–3756 (2007).
[5]A. Giga, Y. Kimoto, Y. Takigawa, and K. Higashi, Scr. Mater. **55**, 143–146 (2006).
[6]S. X. McFadden, R. S. Mishra, R. Z. Valiev, A. P. Zhilyaev, and A. K. Mukherjee, Nature **398**, 684–686 (1999).
[7]D. Wolf, V. Yamakov, S. R. Phillpot, A. Mukherjee, and H. Gleiter, Acta Mater. **53**, 1–40 (2005).
[8]Y. Mishin, M. Asta, and J. Li, Acta Mater. **58**, 1117–1151 (2010).
[9]J. Monk and D. Farkas, Phys. Rev. B **75**, 045414 (2007).
[10]M. Y. Gutkin, I. A. Ovid'ko, and N. V. Skiba, Acta Mater. **51**, 4059–4071 (2003).
[11]D. Farkas, S. Mohanty, and J. Monk, Phys. Rev. Lett. **98**, 165502 (2007).
[12]X. Z. Liao, F. Zhou, E. J. Lavernia, D. W. He, and Y. T. Zhu, Appl. Phys. Lett. **83**, 5062–5064 (2003).
[13]M. Chen, E. Ma, K. J. Hemker, H. Sheng, Y. Wang, and X. Cheng, Science **300**, 1275–1277 (2003).
[14]Z. Shan, E. A. Stach, J. M. K. Wiezorek, J. A. Knapp, D. M. Follstaedt, and S. X. Mao, Science **305**, 654–657 (2004).
[15]G. Wang, J. Lian, Z. Jiang, L. Qin, and Q. Jiang, J. Appl. Phys. **106**, 086105 (2009).
[16]G. Wang, Z. Jiang, H. Zhang, and J. Lian, J. Mater. Res. **23**, 2238–2244 (2008).
[17]A. J. Haslam, S. R. Phillpot, D. Wolf, D. Moldovan, and H. Gleiter, Mater. Sci. Eng. A **318**, 293–312 (2001).
[18]V. Yamakov, D. Wolf, S. R. Phillpot, and H. Gleiter, Acta Mater. **50**, 61–73 (2002).
[19]V. Yamakov, D. Wolf, S. R. Phillpot, A. K. Mukherjee, and H. Gleiter, Nat. Mater. **1**, 45–49 (2002).
[20]V. Yamakov, D. Wolf, M. Salazar, S. R. Phillpot, and H. Gleiter, Acta Mater. **49**, 2713–2722 (2001).
[21]Y. Lu, C. Peng, Y. Ganesan, J. Y. Huang, and J. Lou, Nanotechnology **22**, 355702 (2011).
[22]Z. W. Shan, R. K. Mishra, S. A. Syed Asif, O. L. Warren, and A. M. Minor, Nat. Mater. **7**, 115–119 (2008).
[23]D. Kiener and A. M. Minor, Nano Lett. **11**, 3816–3820 (2011).
[24]D. Kiener and A. M. Minor, Acta Mater. **59**, 1328–1337 (2011).
[25]Y. Zhang, X. Han, K. Zheng, Z. Zhang, X. Zhang, J. Fu, Y. Ji, Y. Hao, X. Guo, and Z. L. Wang, Adv. Funct. Mater. **17**, 3435–3440 (2007).
[26]X. D. Han, K. Zheng, Y. F. Zhang, X. N. Zhang, Z. Zhang, and Z. L. Wang, Adv. Mater. **19**, 2112–2118 (2007).
[27]K. Zheng, C. Wang, Y.-Q. Cheng, Y. Yue, X. Han, Z. Zhang, Z. Shan, S. X. Mao, M. Ye, Y. Yin, and E. Ma, Nat. Commun. **1**, 24 (2010).
[28]L. Wang, X. Han, P. Liu, Y. Yue, Z. Zhang, and E. Ma, Phys. Rev. Lett. **105**, 135501 (2010).
[29]D. F. Stein and J. R. Low, J. Appl. Phys. **31**, 362–369 (1960).
[30]Y. G. Zheng, H. W. Zhang, Z. Chen, C. Lu, and Y. W. Mai, Phys. Lett. A **373**, 570–574 (2009).